Title
Analysis of tropospheric aerosol number density for aerosols of 0.2- to 3-μm diameter: Central and northeastern Canada

Journal
Journal of Geophysical Research, 99(D1)

ISSN
0148-0227

Authors
Gregory, Gerald L
Anderson, Bruce E
Barrick, John D
et al.

Publication Date
1994-01-20

DOI
10.1029/93jd00103

JOURNAL OF GEOPHYSICAL RESEARCH, VOL. 99, NO. D1, PAGES 1757–1762, JANUARY 20, 1994

Analysis of tropospheric aerosol number density for aerosols of 0.2- to 3-μm diameter: Central and northeastern Canada

Gerald L. Gregory, Bruce E. Anderson, and John D. Barrick
Atmospheric Sciences Division, NASA Langley Research Center, Hampton, Virginia

Charles H. Hudgins and Donald R. Bagwell
Operations Support Division, NASA Langley Research Center, Hampton, Virginia

Donald R. Blake
Department of Chemistry, University of California-Irvine, Irvine

Abstract. NASA's Atmospheric Boundary Layer Experiment conducted during the summer of 1990 focused on the distribution of trace species in central and northeastern Canada (altitudes <6 km) and the importance of surface sources/sinks, local emissions, distant transport, tropospheric/stratospheric exchange. Aircraft flights were based from North Bay, Ontario, and Goose Bay, Labrador, Canada. As part of the aircraft measurements, aerosol number density (0.2- to 3-μm diameter) was measured using an optical laser technique. Results show that summertime aerosol budgets of central and northeastern Canada can be significantly impacted by the transport of pollutants from distant source regions. Biomass burning in Alaska and western and central Canada exerts major influences on regional aerosol budgets. Urban emissions transported from the U.S./Canadian border regions are also important. Aerosol enhancements (mixed layer and free troposphere) were most prevalent in air with carbon monoxide mixing ratios >110 parts per billion by volume (ppbv). When data were grouped as to the source of the air (5-day back trajectories) either north or south of the polar jet, aerosol number density in the mixed layer showed a tendency to be enhanced for air south of the jet relative to north of the jet. However, this difference was not observed for measurements at the higher altitudes (4 to 6 km). For some flights, mixed layer aerosol number densities were >100 higher than free-tropospheric values (3- to 6-km altitude). The majority of the observed mixed layer enhancement was associated with transport of effluent-rich air into the Canadian regions. Aerosol emissions from natural Canadian ecosystems were relatively small when compared to transport.

Introduction

Processes occurring in the subarctic and Arctic are believed to have a major impact on global tropospheric chemistry and dynamics [*National Academy of Sciences*, 1984; *Logan*, 1985; *Levy et al.*, 1985; *Gidel and Shapiro*, 1980]. Of particular interest is the extent to which transported emissions from distant source regions, regional/local emissions from biomass burning, subarctic/Arctic boreal and tundra surface emissions, and frequent stratospheric/tropospheric exchange affect regional and global chemical budgets. In the summer the polar front (polar jet) frequently moves north of major populated and industrialized regions [*Rahn and McCaffrey*, 1980], and the degree of north-south migration of the polar jet determines the relative importance of the transport of urban/industrial emissions from the United States and U.S./Canadian border areas to the region. In addition, as the polar jet retreats northward, air transported into Canada can be composed of mixtures from numerous sources, including the Arctic, Pacific Ocean, continental United States/Canada, and Atlantic Ocean. During the summer months, biomass burning influences air on both sides of the polar jet and may equal or exceed any influence of transported urban emissions to the region. As noted by *Shipham et al.* [this issue], the 1990 burning season in Alaska was among the most intense of the past 50 years. Canada's season was relatively inactive with most fires limited to the Yukon and Northwest Territories. The relationship and importance of the various processes are not well known.

Aerosol production (fresh emissions or via heterogenous reactions) is of particular concern because of the importance of aerosols in (1) providing active sites for condensation processes, (2) acting as intermediate products in heterogenous reactions, (3) affecting the Earth's radiative budget, and (4) providing deposition (wet or dry) of pollutants on fragile and sensitive Arctic and subarctic ecosystems. NASA's Arctic Boundary Layer Expedition (ABLE 3B) focused on the distribution of trace species in central and northeastern Canada (altitudes <6 km) and was conducted in the summer of 1990. Aircraft flights were based from North Bay, Ontario, and Goose Bay, Labrador, Canada. This paper discusses the number density (number per cubic centimeters (#/cm^3)) distribution of aerosols measured on the NASA aircraft. Measurements were made in the size

Paper number 93JD00103.
0148-0227/94/93JD-00103$05.00

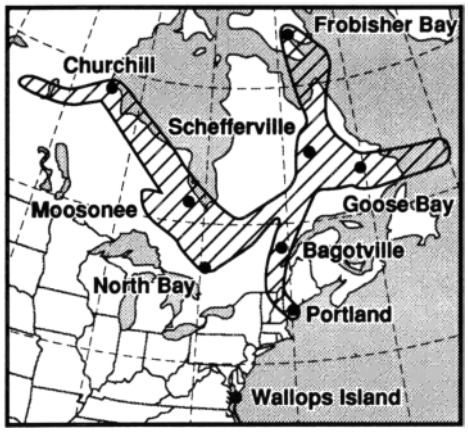

Figure 1. Arctic Boundary Layer Expedition (ABLE) 3B study area.

range of 0.2- to 3-μm diameter using an optical laser technique.

Experimental Techniques

The aircraft platform was the NASA Wallops Electra used in previous ABLE experiments [e.g., *Harriss et al.*, 1988]. The flight plans and a discussion of their scientific objectives are given by *Harriss et al.* [this issue]. Flight plans were selected to provide data for purposes of (1) surface flux studies, (2) latitudinal surveys, (3) trace gas budget studies, and/or (4) photochemistry experiments. Sampling included constant altitude and controlled spiral ascent/descent flights. In general, 5-hour missions were flown covering an altitude range of 150 m to about 6 km above the surface. A total of 22 flights were flown. Figure 1 shows the ABLE 3B study area. Mission 1 was a ferry flight from Virginia (38° N, 75°W) to North Bay, Canada (47° N, 79°W). Flights 2 through 10 were based from North Bay and focused on measurements in the Hudson Bay lowland region and air masses transported into central Canada. Flights 11 through 17 were based from Goose Bay and focused on northeastern Canada and the boreal, peatland, and marine environments. The remaining five flights included (1) a latitudinal survey (free tropospheric and mixed layer) between Goose Bay (53° N, 60° W) and Frobisher Bay (64° N, 69° W) and (2) return flight from Goose Bay to Virginia via Bagotville, Quebec, and Portland, Maine.

The ABLE 3B instrument complement is described by *Harriss et al.* [this issue]. The in situ aerosol package was similar to that used during earlier ABLE missions (see, for example, *Gregory et al.* [1990, 1992]). An active scattering aerosol spectrometer probe (ASASP) (particle measurement system model ASASP-100) mounted external to the aircraft measured aerosol number density (#/cm^3) as a function of time (1-s frequency) and size diameter (0.12- to 3.12-μm diameter). The ASASP sizes aerosols into 15 bins that progressively increase in width (e.g., bin 1, 0.025 μm wide and bin 15, 0.375 μm wide). As a result of an instrument malfunction, data measured in the two smallest bins of the instrument (0.12 to 0.2 μm) are not reported. The aerosol data are averaged over 10-s or 1-min periods. The data have not been corrected for sampling uncertainties [e.g., *Pinnick and Auvermann*, 1979; *Patterson et al.*, 1980; *Garvey and Pinnick*, 1983; *Dye and Baumgardner*, 1984; *Pinnick et al.*, 1981], and the size bin calibration of the probe was performed by the manufacturer. Data measured during takeoff and landing and sampling within clouds are excluded from the analyses.

Aerosol Number Density Results

General Observations

Figure 2 shows fine aerosol (0.2- to 3-μm diameter) histograms for the data when grouped as free troposphere (3- to 6-km altitude) and mixed layer (<300 m above ground level). No distinctions were made in the grouping for the type of underlying terrain, air mass source, or meteorological condition. The data are from flights 2 through 19 and exclude the ferry flights between Canada and the United States. Statistics for each grouping are given in the panels. The maximum aerosol number density of 359 shown in the statistics panel of Figure 2*a* and the average number density shown as a factor of 5 higher than the median value are the direct result of data from a single flight (flight 6). As discussed later, flight 6 measurements were heavily influenced by biomass burning occurring in Alaska.

The median for the mixed layer (ML) aerosol loadings is about 20 times higher (44 as compared to 2/cm^3) than those of the free troposphere (FT). Use of the median of the observations to represent the results instead of the average reduces the influence of single observations which may not be representative of the grouping. ABLE 3A measurements (same altitude bands and aerosol size ranges) in the Alaskan

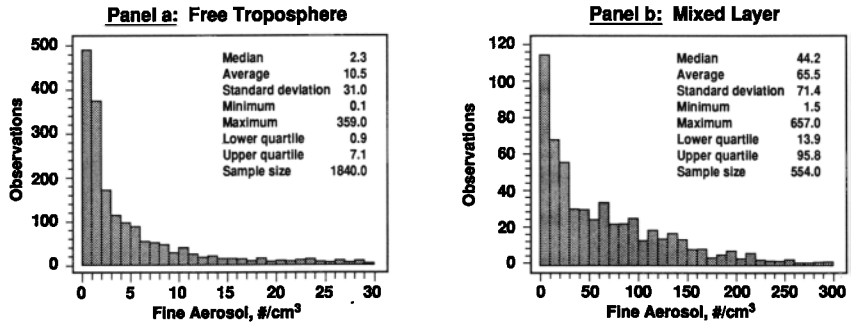

Figure 2. Number density histograms. Free-tropospheric data are for measurements at altitudes of 3 to 6 km. Mixed layer data are for altitudes <300 m above the surface. Fine aerosol is defined as aerosol diameters in the range of 0.2 to 3 μm.

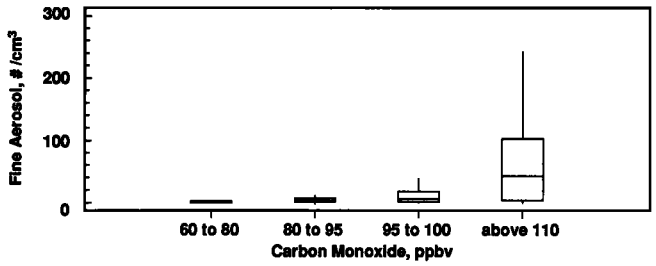

Figure 3. Comparison of ABLE 3B aerosol number densities (0.2- to 3-μm diameter) as a function of carbon monoxide (CO) mixing ratio. Data are grouped into four CO mixing ratio ranges. For each range the box encompasses 50% of the observations (box boundaries are the upper and lower quartile ranges); the horizontal line (within the box) notes the median of the data; and the whiskers (vertical lines extending from the box) represent the extremes of the data or in cases where there are values some distance from the bulk of the data, they extend to a value equal to 1.5 times the interquartile values.

ML over dry tundra (Barrow region) or wet tundra (Bethel region) showed (ML)/(FT) ratios of the order of 1.5 to 2.5 when FT air was from continental polar regions (Siberian, Canadian, or Arctic sources as determined from 5-day back trajectory analyses). The expression (ML)/(FT) is defined as the median ML number density for a data grouping (e.g., flight 2) divided by the median FT number density for the same data grouping.

Figures 3 and 4 provide an indication as to the general nature of the air in which enhanced levels of aerosol were measured. Figure 3 is a box-and-whisker plot of the ABLE 3B 10-s-averaged aerosol data and includes measurements at all altitudes. The box-and-whisker format is explained in the figure legend. For the analyses the aerosol data are grouped into four categories depending upon the level of carbon monoxide (CO) measured: (1) 60 to 80 parts per billion by volume (ppbv), (2) 80 to 95, (3) 95 to 100, and (4) >110 ppbv. As shown, the majority of aerosol enhancement occurred in air with CO mixing ratios >110 ppbv. The median altitude of the aerosol measurements for the four CO bands ranged from 3 to 4 km, thus eliminating CO variance with altitude as a cause for the trend seen in Figure 3. As discussed by several ABLE 3B investigators [e.g., *Talbot et al.*, this issue; *Sandholm et al.*, this issue], air masses with CO values above about 100 to 110 ppbv were generally associated with biomass burning and/or urban combustion emissions.

For the analyses of Figure 4 the aerosol data are grouped using the meteorological analyses of *Shipham et al.* [this issue] according to whether the source of the air (5-day back trajectory) was north of the polar jet (Figure 4*a*, polar air) or south of the jet (Figure 4*b*, mid-latitude air). Methods used to construct the isentropic back trajectories are discussed by *Shipham et al.* [this issue]. In each panel, two subgroupings are shown: (1) air sampled at potential temperatures of 310° to 320° C (altitudes of 4 to 6 km) and (2) air sampled in the ML layer at 290° to 295° C (<1 km). While both the polar and the mid-latitude groupings show an increase in ML aerosols (compared to FT), the factor of about 100 increase (Figure 4*b*, median values) for mid-latitude air compared to only a factor of 10 for polar air (Figure 4*a*) shows that the increase in ML aerosol observed in Figure 2 occurred mostly in air from sources south of the polar jet.

Figure 4*c* compares the polar and mid-latitude free tropo-

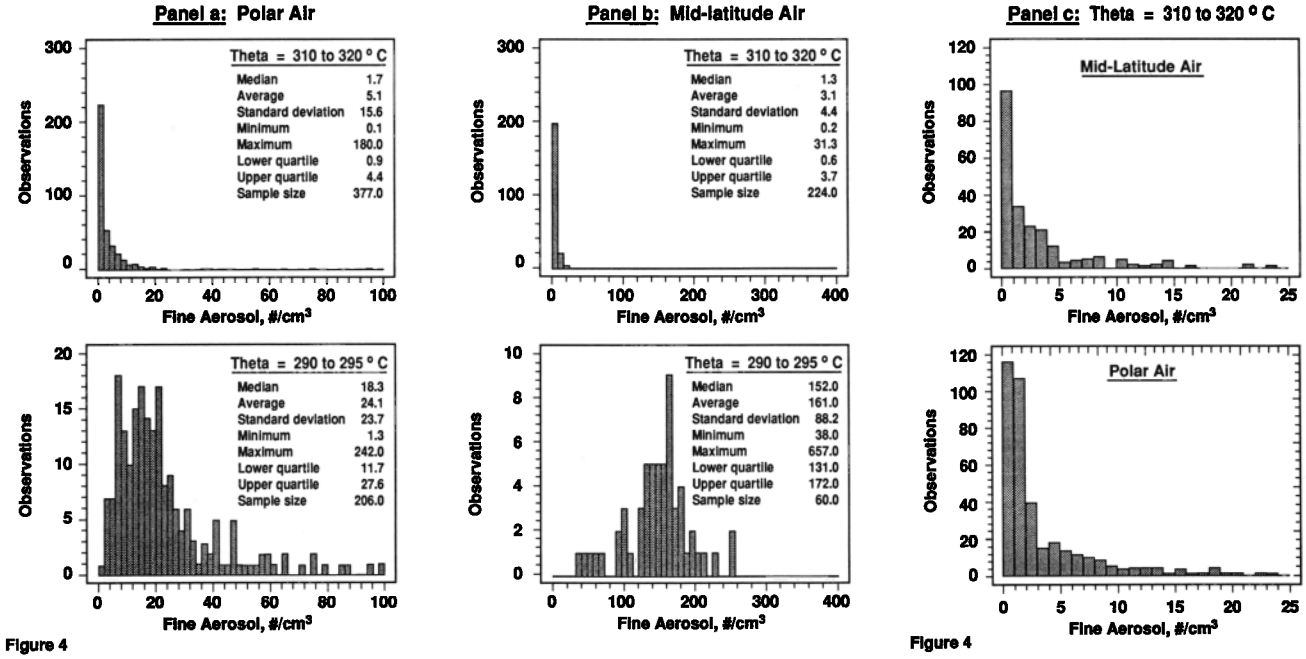

Figure 4

Figure 4

Figure 4. Aerosol number density results (0.2- to 3-μm diameter) for ABLE 3B data grouped according to the potential temperature of the air at the time of sampling. Potential temperatures (theta) of 310° to 320° C equate to free-tropospheric measurements at altitude above about 4 to 5 km; theta of 290° to 295° C relate to mixing layer measurements at about 1-km altitude. The following are shown: (a) results for polar source air or air which originated (5-day trajectory) north of the polar jet and (b) results for mid-latitude source air (south of the polar jet). (c) Comparison (x axes expanded) of the 310° to 320° potential temperature data grouping of (a) and (b).

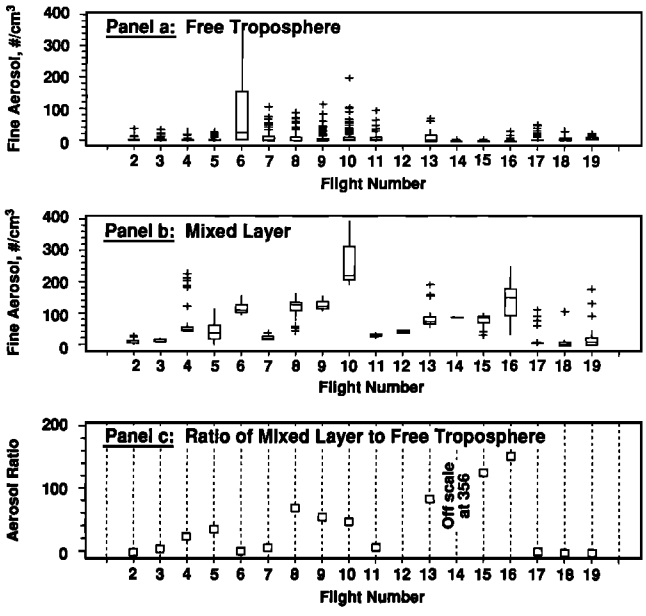

Figure 5. Comparison of ABLE 3B aerosol number densities (0.2- to 3-μm diameter) on a flight basis. The data are grouped as free troposphere (measurements >3-km altitude) and mixed layer (<300 m above the surface). (a and b) Box-and-whisker format. The box encompasses 50% of the observations (box boundaries are the upper and lower quartile ranges); the horizontal line (within the box) notes the median of the data; the whiskers (vertical lines extending from the box) represent the extremes of the data or in cases where there are values some distance from the bulk of the data, they extend to a value equal to 1.5 times the interquartile values; and extreme values beyond the whiskers are plotted with the "plus" symbol. (c) Plot of the ratio of the median values of (b), mixed layer, to (a), free troposphere, i.e., aerosol ratio = (ML)/(FT); see text.

spheric data (potential temperatures of 310° to 320°) of Figures 4*a* and 4*b* where the *x* axis scale has been expanded. As shown by this comparison, aerosol loadings above about 4 to 6 km are similar whether the air was from sources south or north of the polar jet. In fact, comparison of the total chemical signature (CO, nitrogen oxides, nonmethane hydrocarbons, fluorocarbons, etc.) for the same data groupings also showed little difference at the higher altitudes.

Specific Processes

The results from Figures 3 and 4 provide some information into the general nature of air that was observed to be enhanced in aerosol. The data of Figure 5 in combination with back trajectory analyses [*Shipham et al.*, this issue] provide insight into the relative magnitude of specific processes which are important to aerosol loadings in the Canadian regions. Figure 5 shows data on a flight-by-flight basis. The FT data correspond to measurements above 3-km altitude (same as Figure 2). Data above 3-km altitude are not available for flight 12. The ML data have been expanded to include measurements at altitudes <1 km as compared to <300 m used for Figure 2. This was necessary as some flights did not have sufficient sampling below 300-m altitude to allow box-and-whisker analyses. Figures 5*a* and 5*b* are box-and-whisker plots for the FT and ML results, respectively. Figure 5*c* plots the ratio of the median ML aerosol loading (Figure 5*b*) to the median FT loading (Figure 5*a*), i.e., (ML)/(FT).

Polar source, background air. As discussed by *Shipham et al.* [this issue] and *Anderson et al.* [this issue], the column of air (surface to about 6-km altitude) at any location and time was generally not from a single source but was often composed of mixtures of polar and mid-latitude air each influenced by different types of emissions. However, air mass trajectories for flights 2, 3, 18, and 19 suggested polar source air at all altitudes with little modification during transport via biomass burning or urban pollution. As shown in Figures 5*a* and 5*b*, FT and ML aerosol number densities for these flights are among the lowest observed. In addition, the ratio of ML to FT loadings (Figure 5*c*) are also among the lowest (ratios (ML)/(FT)) for the individual flights ranged from 1.5 to 7; average of the ratio for the four flights was about 3). As a result and for ABLE 3B data only, we interpret (ML)/(FT) ratios below about 7 as suggesting that the increase in ML aerosol loading (compared to FT) is mostly the result of thermodynamic processes (higher air density and humidity of the ML samples compared to FT), mechanical processes (the presence of wind-blown surface elements in the mixed layer), and/or natural emissions from the underlying ecosystem. (ML)/(FT) ratios as large as a factor of 1.5 to 2 can be expected to occur due to differences in air density for the two altitude ranges.

Canadian ecosystems. Mixed layer aerosol results for flights 2, 3, and 17 illustrate the aerosol production associated with natural Canadian ecosystems. ML data for these flights were mostly low-altitude (150 to 300 m) samplings over remote Hudson Bay lowlands (flights 2 and 3) or eastern Canadian wetland/forest (flight 17) ecosystems during periods in which the air was not significantly impacted by urban or biomass-burning emissions. As noted above, FT air for flights 2 and 3 was of polar origin. FT air for flight 17 was of split origin, consisting of mixtures of polar air similar to flights 2 and 3, north central Canadian air, and air exposed to urban emissions from the Great Lakes region. As shown in Figure 5*a*, FT aerosol number densities are relatively low for all three flights as are the (ML)/(FT) ratios. (ML)/(FT) ratios for the flights ranged from 3 (flights 2 and 17) to 7 (flight 3). For comparison, similar ratios observed in Alaska during ABLE 3A were 15 (boreal forest, Brooks Mountain Range region) and 6 (wet tundra, Bethel region).

Influences of biomass-burning emissions. Flights 6, 7, 8, 9, and 11 were influenced by biomass-burning emissions. For flights 6, 7, and 11 the source region of the biomass-burning emissions was primarily from Alaska (3 to 5 days old), while for flights 8 and 9, emissions were from central Canada (12 to 24 hours old). As illustrated in Figure 5*a*, FT aerosol loading does not vary significantly among flights, with the exception of flight 6. While the FT loading for flight 6 is relatively high (median of 27/cm^3), the ratio of ML to FT loading (Figure 5*c*) is low ((ML)/(FT) = 4) and compares well to those of flights 2, 3, 18, and 19. Thus the increase in aerosol observed for the mixed layer during flight 6 is mostly the result of the higher FT loadings and natural processes (see earlier discussions) acting on the aerosols as they descended to lower altitudes. Similarly for the aged biomass-burning emissions associated with flights 7 and 11, (ML)/(FT) ratios are low (about 10). However, for flights 8 and 9 (younger emissions), ratios are of the order of 50 to 60. The higher (ML)/(FT) ratios observed for flights 8 and 9 (relative to flights 6, 7, and

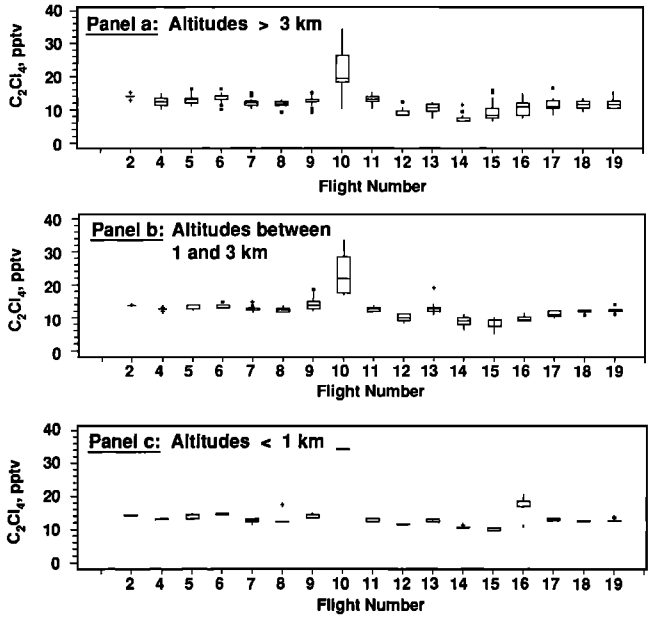

Figure 6. Box-and-whisker plots of ABLE 3B carbon tetrachloride (C_2Cl_4) data. C_2Cl_4 is a tracer of urban emissions. The measurements are grouped into three altitude ranges: (a) includes measurements made above 3 km, (b) 1 to 3 km, and (c) <1 km. The box-and-whisker format is explained in the legend of Figure 5. Where insufficient data are available from a given flight for the box-and-whisker analyses, the median of the data is plotted as a horizontal line.

11) are consistent with the emissions not having sufficient time to have mixed into the FT and in situ aerosol production occurring within the mixed layer during transport of the younger and more chemically active emissions. Since the background air for flight 6 was from polar sources, results from flight 6 best illustrate the sizable impact that transported biomass-burning emissions can have on regional Canadian aerosol budgets.

Influence of urban emissions. The highest ML aerosol loadings of Figure 5 are clearly those of flight 10 (median of 224) and included measurements in air transported (2 to 3 days) from industrialized regions of the United States and the U.S./Canadian border. Flights 4, 5, 13, and 16 were also influenced (lesser degree) by urban emissions as well as being affected by biomass-burning emissions. The (ML)/(FT) ratios for the urban-influenced flights range from 27 to 120 (flight 10 = 49). Again, the large ratios can be attributed to insufficient time for mixing to FT altitudes and/or in situ aerosol production during transport in the mixed layer.

Figure 6 shows box-and-whisker plots of the urban tracer C_2Cl_4. Data are given for three altitude bands: >3 km, 1 to 3 km, and <1 km. The relatively high values of C_2Cl_4 for flight 10 confirms the primarily urban influence of flight 10 compared to the other flights. In addition, the elevated C_2Cl_4 measured in samples above 3-km altitude (Figure 6*a*) suggests that at least for flight 10, urban emissions had time to mix to FT altitudes, and thus the observed (ML)/(FT) ratio of 49 for flight 10 is probably due to in situ aerosol production in the mixed layer during transport.

Tropical source air. Tropical air from the Pacific Ocean was sampled during large segments of the FT sampling of flights 14 and 15. As discussed by *Shipham et al.* [this issue], the air originated 10 to 15 days earlier from the outflow of Typhoon Steve located in the western Pacific. The tropical air was transported at FT altitudes into the sampling region without significant modification by biomass burning or urban emissions, stratospheric/tropospheric exchange, or mixing of ML air into the FT. *Browell et al.* [this issue] indicate that the clean tropical air extended from just above the mixed layer to near the tropopause. *Anderson et al.* [this issue] report ozone values of 20 ppbv for the tropical air, while *Talbot et al.* [this issue] report low values of CO (~60 ppbv), CH_4 (~1700 ppbv), and NO_y (~200 parts per trillion by volume (pptv)).

FT aerosol number density for these flights was the lowest observed during ABLE 3B: 0.3/cm^3 (flight 14) and 0.7/cm^3 (flight 15), as compared to a median number density for all the flights of 2.3 (Figure 2*a*). The high (ML)/(FT) ratio for flights 14 and 15 shown in Figure 5*c* are largely due to the low aerosol content of the FT tropical air. (ML)/(FT) ratios of 350 (flight 14) and 125 (flight 15) are reduced to 45 and 38, respectively, when 2.3/cm^3 (median of all flights) is used as the FT number density. However, even these ratios are high and, as shown in Figure 5*b*, ML number densities are relatively high compared to some of the flights (e.g., polar background air of flights 2, 3, 18, and 19). The source of the ML air (5-day back trajectory) was from north central Canada and Arctic regions with passage over the Hudson Bay 1 to 2 days prior to sampling. No evidence of biomass burning or urban influence is seen from the trajectory analyses. The higher ML loading is believed to be the result of marine influences as the air passed over the Hudson Bay. The aerosol sizing data tend to support the marine hypothesis but are not conclusive as the result of the lost data in the first two bins of the instrument.

Concluding Remarks

Analyses of aerosol number density data (0.2- to 3-μm diameter) showed that the aerosol budgets of central and northeastern Canada are significantly impacted by the transport of pollutants from distant source regions. In particular, biomass burning in Alaska and western and central Canada exerts a major influence on regional aerosol budgets. Urban emissions transported from the U.S./Canadian border regions are also important.

In all cases, mixed layer aerosol number densities exceeded those of the free troposphere by factors of 1.3 to above 100. The highest mixed layer aerosol loadings (e.g., 100 to 200/cm^3) occurred in air influenced by distant pollution and emissions which were transported into the Canadian regions. When polar source air was relatively clean and devoid of influences from transported emissions, mixed layer number densities were in the range of about 5 to 10/cm^3 and mixed layer aerosol loadings were only about a factor of 3 higher than free-tropospheric values, of which a factor of 1.5 to 2 can be attributed to air density differences of the samples at the different altitudes.

When data were grouped according to the carbon monoxide levels measured in the air, the majority of aerosol enhancements occurred in air with CO >110 ppbv. When data were grouped as being measured in air which was from sources either south (mid-latitude) or north (polar) of the polar jet, the ratio of mixed layer to free-tropospheric

number densities averaged about a factor of 100 (mid-latitude) compared to factors of only 10 for air north of the jet. While mid-latitude mixed layer air showed a tendency to be enriched in aerosols (compared to polar air), both mid-latitude and polar air showed similar aerosol loadings at the higher altitudes (e.g., 4 to 6 km).

The highest free-tropospheric aerosol loadings (3- to 6-km altitude) observed during ABLE 3B occurred in polar air which was influenced by Alaskan biomass-burning emissions injected into the air 4 to 5 days prior to sampling. Associated with the higher free-tropospheric loadings was a sizable increase in mixed layer loadings. However, mixed layer to free-tropospheric number density ratios were only about a factor of 4 (similar to polar background air) and thus the high mixed layer loadings were the result of aerosol-enriched, free-tropospheric air having been transported into the sampling region.

Acknowledgments. The authors wish to acknowledge the NASA Wallops ground and flight crews for their suggestions and cooperation during the flights and, in particular, Roger Navarro (aircraft coordinator). We thank Arnold Torres and his staff at Wallops for providing an independent verification of the calibration of the ozone detectors. Lastly, we acknowledge and appreciate the hospitality of local officials and citizens of North Bay and Goose Bay, Canada.

References

Anderson, B. E., G. L. Gregory, J. D. Barrick, J. E. Collins, G. W. Sachse, and M. Shipham, Summertime tropospheric ozone distributions over central and eastern Canada, *J. Geophys. Res.*, this issue.

Browell, E. V., M. A. Fenn, C. F. Butler, W. B. Grant, R. C. Harriss, and M. C. Shipham, Ozone and aerosol distributions in the summertime troposphere over Canada, *J. Geophys. Res.*, this issue.

Dye, J. E., and D. Baumgardner, Evaluation of the forward scattering spectrometer probe, I, Electronic and optical studies, *J. Atmos. Oceanic Technol.*, *1*, 329–344, 1984.

Garvey, D. M., and R. G. Pinnick, Response characteristics of the Particle Measuring Systems active scattering aerosol spectrometer probe (ASASP-X), *Aerosol Sci. Technol.*, *2*, 477–488, 1983.

Gidel, L. T., and M. A. Shapiro, General circulation model estimates of the net vertical flux of ozone in the lower stratosphere and the implications for the tropospheric ozone budget, *J. Geophys. Res.*, *85*, 4049–4058, 1980.

Gregory, G. L., E. V. Browell, L. S. Warren, and C. H. Hudgins, Amazon basin ozone and aerosol: Wet season observations, *J. Geophys. Res.*, *95*, 16,903–16,912, 1990.

Gregory, G. L., B. E. Anderson, L. S. Warren, E. V. Browell, D. R. Bagwell, and C. H. Hudgins, Tropospheric ozone and aerosol observations: The Alaskan Arctic, *J. Geophys. Res.*, *97*, 16,451–16,471, 1992.

Harriss, R. C., et al., The Amazon Boundary Layer Experimkent (ABLE 2A): Dry season, 1985, *J. Geophys. Res.*, *93*, 1351–1360, 1988.

Harriss, R. C., et al., The Arctic Boundary Layer Expedition (ABLE-3B): July to August 1990, *J. Geophys. Res.*, this issue.

Levy, H., II, J. D. Mahlman, W. J. Moxim, and S. C. Liu, Tropospheric ozone: The role of transport, *J. Geophys. Res.*, *90*, 3753–3772, 1985.

Logan, J. A., Tropospheric ozone: Seasonal behavior, trends, and anthropogenic influence, *J. Geophys. Res.*, *90*, 10,463–10,482, 1985.

National Academy of Sciences, *Global Tropospheric Chemistry: A Plan for Action*, 194 pp., National Academy Press, Washington, D. C., 1984.

Patterson, E. M., C. S. Kiang, A. C. Delany, A. W. Wartburg, A. C. Leslie, and B. J. Huebert, Global measurement of aerosol in remote continental and marine regions: Concentrations, size distributions and optical properties, *J. Geophys. Res.*, *85*, 7361–7376, 1980.

Pinnick, R. G., and H. J. Auvermann, Response characteristics of Knollenberg light-scattering aerosol counters, *J. Aerosol Sci.*, *10*, 55–74, 1979.

Pinnick, R. G., D. M. Garvey, and L. D. Duncan, Calibration of Knollenberg FSSP light scattering counters for measurement of cloud droplets, *J. Appl. Meteorol.*, *20*, 1049–1057, 1981.

Rahn, K. A., and R. J. McCaffrey, On the origin and transport of winter Arctic aerosol, *Ann. N. Y. Acad. Sci.*, *338*, 486–503, 1980.

Sandholm, S. J., et al., Summertime partitioning and budget of NO_y compounds in the troposphere over Alaska and Canada: ABLE 3B, *J. Geophys. Res.*, this issue.

Shipham, M. C., A. S. Bachmeier, D. R. Cahoon, Jr., G. L. Gregory, B. E. Anderson, and E. V. Browell, A meteorological interpretation of the Arctic Boundary Layer Expedition (ABLE) 3B flight series, *J. Geophys. Res.*, this issue.

Talbot, R. W., et al., Summertime distributions and relations of reactive odd nitrogen species and NO_y in the troposphere over Canada, *J. Geophys. Res.*, this issue.

B. E. Anderson, J. D. Barrick, and G. L. Gregory, Atmospheric Sciences Division, NASA Langley Research Center, Hampton, VA 23681-0001.

D. R. Bagwell and C. H. Hudgins, Operations Support Division, NASA Langley Research Center, Hampton, VA 23681-0001.

D. R. Blake, Department of Chemistry, University of California-Irvine, Irvine, CA 92664.

(Received August 14, 1992; revised December 31, 1992; accepted December 31, 1992.)